NEURAL NETWORK MODELING OF UH-60A PILOT VIBRATION

Sesi Kottapalli
Army/NASA Rotorcraft Division
NASA Ames Research Center
Moffett Field, California
E-mail: Sesi.B.Kottapalli@nasa.gov

Abstract

Full-scale flight-test pilot floor vibration is modeled using neural networks and full-scale wind tunnel test data for low speed level flight conditions. Neural network connections between the wind tunnel test data and the three flight test pilot vibration components (vertical, lateral, and longitudinal) are studied. Two full-scale UH-60A Black Hawk databases are used. The first database is the NASA/Army UH-60A Airloads Program flight test database. The second database is the UH-60A rotor-only wind tunnel database that was acquired in the NASA Ames 80- by 120-Foot Wind Tunnel with the Large Rotor Test Apparatus (LRTA). Using neural networks, the flight-test pilot vibration is modeled using the wind tunnel rotating system hub accelerations, and separately, using the hub loads. The results show that the wind tunnel rotating system hub accelerations and the operating parameters can represent the flight test pilot vibration. The six components of the wind tunnel N/rev balance-system hub loads and the operating parameters can also represent the flight test pilot vibration. The present neural network connections can significantly increase the value of wind tunnel testing.

Notation

C_T	Rotor thrust coefficient
C_W	Helicopter gross weight coefficient
LRTA	Large Rotor Test Apparatus
MISO	Multiple-input, single-output
N	Number of main rotor blades, N = 4 for the UH-60A
N/rev	Integer (N) multiple of main rotor speed
PLATV	Peak, N/rev pilot floor lateral vibration, g's
PLONGV	Peak, N/rev pilot floor longitudinal vibration, g's
PVV	Peak, N/rev pilot floor vertical vibration, g's
R	Linear regression correlation
RMS error	Root mean square error, g's
α_s	Rotor shaft angle measured from vertical, positive aft, deg
σ	Rotor solidity ratio

Presented at the AHS 4th Decennial Specialist's Conference on Aeromechanics, San Francisco, California, January 21-23, 2004.

Introduction

At present, helicopter vibration levels cannot be predicted with confidence. The relationships between the helicopter rotor hub accelerations and the corresponding fuselage vibration may be linear or nonlinear, and involve many variables. Here, fuselage vibration is defined as the N/rev fuselage acceleration at the pilot floor location where N is the number of blades. Using only flight test data, neural networks were used to connect the flight test rotating system hub accelerations to the flight test pilot vibration (Refs. 1 and 2). The current study uses neural networks to connect ground based wind tunnel data to the flight test pilot vibration in low speed level flight. Neural network relationships between the wind tunnel data and the three flight test pilot floor vibration components (vertical, lateral, and longitudinal) are studied in this paper. A recent initial study (Ref. 3) had considered only the pilot floor vertical vibration component.

This neural network study introduces the use of ground-based wind tunnel test data to model the pilot floor vibration in flight. Two full-scale UH-60A Black Hawk databases are used. The first database is the NASA/Army UH-60A Airloads Program flight test database (Ref. 4). The second database is the low speed full-scale UH-60A rotor-only wind tunnel database (Refs. 5-7) that was acquired in the NASA Ames 80- by 120-Foot Wind Tunnel with the Large Rotor Test Apparatus (LRTA). The successful establishment of

such neural network based connections (relationships) between the wind tunnel parameters and the flight test data can increase the value of wind tunnel testing. This is because wind tunnel testing is less expensive than flight testing and a range of steady flight conditions can be easily explored. In the present study, the measured wind tunnel parameters under consideration include both rotating system parameters (hub accelerations) and fixed system parameters (hub loads from the dynamic rotor balance system).

Using neural networks and flight test data, it was shown earlier (Refs. 1 and 2) that the flight test hub accelerations plus the advance ratio and gross weight could be used to model the flight test pilot floor vibration. It was shown in Ref. 3 that the wind tunnel and flight test data of interest have similar trends (Fig. 1 of Ref. 3). Based on the above noted similarity, the present neural network study proceeds to establish the connections between the wind tunnel hub accelerations and the flight test pilot floor vibration in low speed level flight. Subsequently, this study also considers additional wind tunnel data such as the fixed system rotor-generated balance-system loads.

The focus of future work is to extend the present study to predict the flight test pilot vibration with active controls using the available wind tunnel data.

Objectives

The general objective of this study is to evaluate the potential of using wind tunnel measurement to represent flight vehicle vibrations using neural networks. The present study has the following four specific objectives:

1. Using the flight test advance ratio and gross weight, obtain low speed, neural network based models of the PVV, the PLATV, and the PLONGV.

2. Using the measured wind tunnel rotating system hub accelerations and operating parameters, determine whether reasonably accurate neural network based models of the flight test PVV, PLATV, and PLONGV can be obtained.

3. Using the measured six components of the wind tunnel fixed system N/rev balance hub loads and the operating parameters, determine whether reasonably accurate neural network models of the PVV, the PLATV, and the PLONGV can be obtained.

4. Assess the results to determine whether a particular approach is markedly better than the others to predict the flight test measurements or whether alternative wind tunnel test measurements would be required.

Flight Test and Wind Tunnel Databases

The source of the flight test data was the NASA/Army UH-60A Airloads Program flight test database (Ref. 4). The flight test data were obtained with the bifilar vibration absorbers installed on the UH-60A. The creation of the pilot floor vibration components (PVV, PLATV, and PLONGV) database has been described separately (Refs. 1 and 2). The present study considers the flight test rotating system hub accelerometers. Specifically, the (N-1)P and the (N+1)P tangential (in-plane) hub accelerations and the NP vertical hub acceleration are considered. The number of flight test data points that are of present interest is 47 (low speed level flight conditions).

The low speed full-scale UH-60A wind tunnel database (Refs. 5-7) that was acquired in the NASA Ames 80- by 120-Foot Wind Tunnel with the Large Rotor Test Apparatus (LRTA) is used. The bifilar vibration absorbers were not installed during this test. The present study considers the (N-1)P and the (N+1)P tangential (in-plane) hub accelerations and the NP vertical hub acceleration. Also, the six components of the N/rev hub loads from the LRTA dynamic rotor balance-system are considered (normal force, axial force, side force, pitching moment, rolling moment, and yawing moment). Sixty-two wind tunnel data points were used in this study. These wind tunnel data points include variations in advance ratio, thrust coefficient, and shaft angle (the variations in the shaft angle allow for simulation of flight conditions that include level flight, climb and descent conditions).

Procedurally, the wind tunnel and the flight test operating conditions are matched in a simple manner. The wind tunnel and flight test advance ratios are matched, and the flight test C_W/σ and the wind tunnel $(C_T\cos\alpha_s)/\sigma$ are matched. The above approach of relating the wind tunnel variables to the flight test variables is believed to be an adequate approach for this initial study that includes all three pilot floor vibration components.

Basic Variations

Figures 1-3 show the low-speed level-flight variations of the flight test pilot vibration with advance ratio. In addition to the variation in the advance ratio covered in these figures, these data involve variations in C_W/σ.

The measured, subject wind tunnel data were shown in Ref. 3 (Figs. 2-5 of Ref. 3) and are not included in this paper. The wind tunnel measurements include the rotating system hub accelerations and the fixed system hub loads. The wind tunnel database contains 62 points. In addition to the variation in the advance ratio, the wind tunnel data involve variations in C_T and α_s. As a result,

many of the wind tunnel operating conditions do not simulate level flight. The measured wind tunnel data were previously validated in Ref. 3, i.e., an assessment of the quality of the wind tunnel was performed and the data were found to be of good quality.

In this paper, the rotating system (N-1)P and (N+1)P tangential (in-plane) hub accelerations and the NP vertical hub acceleration are referred to as the "three relevant" hub acceleration components. Also, the wind tunnel advance ratio and $(C_T \cos\alpha_s)/\sigma$ are referred to as the wind tunnel operating condition parameters (the "operating parameters"). This neural network based modeling study considers low speed level flight conditions and does not include the hover condition.

Neural Network Approach

The overall neural network modeling approach is given in Ref. 1. To accurately capture the required functional dependencies, the neural network inputs must be carefully selected and account for all important physical traits that are specific to the application. The back-propagation type of network with one hidden layer, a hyperbolic tangent as the basis function, and the extended-delta-bar-delta (EDBD) algorithm as the learning rule (Ref. 8) is used in this study. The required number of neural network processing elements (PEs) depends on the specific application. The determination of the appropriate number of PEs is done by starting with a minimum number of PEs. Additional PEs are added to improve neural network performance by reducing the RMS error between the test data and the neural network predictions.

For the notation used in this paper, a neural network architecture such as "2-3-1" refers to a neural network with two inputs, three processing elements in the single hidden layer, and one output. This application of neural networks has been conducted using the neural networks package NeuralWorks Pro II/PLUS (version 5.51) by NeuralWare (Ref. 8).

Results

This neural network study separately considers the three components of the N/rev pilot floor vibration, namely, the vertical component, PVV, and the two in-plane components, PLATV and PLONGV. In the present study, the flight test pilot floor vibration is predicted using neural networks and measured ground based wind tunnel data. The measured wind tunnel data include the three relevant rotating system hub accelerations and separately, the fixed system N/rev balance-system hub loads. In this study, the neural network training results (the correlation results) are presented along with the following two parameters, the linear regression correlation "R," where an "R" close to 1 indicates that a regression-based relationship exists between the test data and the neural network predictions, and the RMS error.

Since the actual flight test PVV, PLATV, and PLONGV values are originally from the 47-point flight test database, for present purposes, the appropriate values of the PVV, PLATV, and PLONGV have to be obtained at the 62-point wind tunnel operating condition values. The pilot floor vibration components at the wind tunnel operating conditions are referred to as the "flight test PVV," the "flight test PLATV," and the "flight test PLONGV." These flight test values are obtained as described in the following section.

Pilot vibration from flight test advance ratio and gross weight

Three different MISO 2-3-1 back-propagation neural networks are trained from the three 47-point flight test databases (one for each of the three vibration components). The two inputs are as follows: the flight test advance ratio and C_W/σ. The single output is the actual, respective pilot floor vibration value (PVV or PLATV or PLONGV). For PVV, the above back-propagation network has been trained for 300,000 iterations with resulting R = 0.754 and RMS error = 0.019 g's. For PLATV, the above back-propagation network has been trained for 10,000 iterations with resulting R = 0.626 and RMS error = 0.024 g's. For PLONGV, the above back-propagation network has been trained for 200,000 iterations with resulting R = 0.860 and RMS error = 0.019 g's. Figures 4-6 show the resulting correlation plots for the PVV, PLATV, and PLONGV, respectively. Figures 4-6 show that, for purposes of this initial study, the advance ratio and the gross weight can reasonably predict the low speed pilot floor vibration. Representative parametric variations of the pilot floor vibration components have been obtained by executing the above three trained back-propagation networks with varying inputs (advance ratio and weight coefficient/solidity ratio). The resulting neural network predictions display consistent trends and are shown in Figs. 7-9. Figures 7-9 show the low speed, neural network predicted parametric variations of the PVV (Fig. 7), the PLATV (Fig. 8), and the PLONGV (Fig. 9) versus the advance ratio for a weight coefficient/solidity ratio range 0.07 to 0.13 and an advance ratio range 0.09 to 0.19.

Figures 10-12 show the flight test PVV (Fig. 10), PLATV (Fig. 11), and PLONGV (Fig. 12) variations with the advance ratio where the respective neural network has been executed using the wind tunnel operating parameters as the inputs (62 points).

The following sections describe three different methods of predicting the pilot floor vibration. The first method uses the flight test rotating system hub accelerations.

The second method uses the measured wind tunnel rotating system hub accelerations, and the third method uses the measured wind tunnel fixed system N/rev balance-system hub loads. In this paper, representative, predicted pilot floor vibration variations with advance ratio for C_W/σ (or equivalently, $(C_T\cos\alpha_s)/\sigma$) = 0.08 are presented.

Pilot vibration prediction using flight test rotating system hub accelerations

Three different MISO 5-6-1 back-propagation neural networks are used (one for each of the three vibration components). The five flight test inputs are as follows: the three relevant actual flight test rotating system hub accelerations, the advance ratio, and C_W/σ. The single output is the actual, respective pilot floor vibration value (PVV or PLATV or PLONGV). For PVV, the above back-propagation network has been trained for 3 million iterations with resulting R = 0.991 and RMS error = 0.004 g's. For PLATV, the above back-propagation network has been trained for 3 million iterations with resulting R = 0.979 and RMS error = 0.006 g's. For PLONGV, the above back-propagation network has been trained for 820,000 iterations with resulting R = 0.994 and RMS error = 0.004 g's. The three correlation plots and the predictions for the three pilot floor vibration components are presented as follows.

PVV from flight test hub accelerations. Figure 13a shows the correlation plot for the PVV using the flight test hub accelerations. Figure 13b shows the representative, predicted PVV using the flight test hub accelerations and the flight test PVV derived from Fig. 10 (from the neural network used to obtain Fig. 10). In Fig. 13b, the two PVV variations with advance ratio (at constant thrust) show similar trends, namely, showing first an increase in the pilot floor vertical vibration with advance ratio and subsequently showing a decrease in the pilot floor vertical vibration with advance ratio.

PLATV from flight test hub accelerations. Figure 14a shows the correlation plot for the PLATV using the flight test hub accelerations. Figure 14b shows the representative, predicted PLATV using the flight test hub accelerations and the flight test PLATV derived from Fig. 11 (from the neural network used to obtain Fig. 11). In Fig. 14b, the two PLATV variations with advance ratio (at constant thrust) show similar trends, namely, a decrease in the pilot floor lateral vibration with advance ratio.

PLONGV from flight test hub accelerations. Figure 15a shows the correlation plot for the PLONGV using the flight test hub accelerations. Figure 15b shows the representative, predicted PLONGV using the flight test hub accelerations and the flight test PLONGV derived from Fig. 12 (from the neural network used to obtain Fig. 12). In Fig. 15b, the two PLONGV variations with advance ratio (at constant thrust) show similar trends, namely, a decrease in the pilot floor longitudinal vibration with advance ratio.

Pilot vibration prediction using wind tunnel rotating system hub accelerations

Three different MISO 5-2-1 back-propagation neural networks are used (one for each of the three vibration components). The five wind tunnel inputs are as follows: the three relevant wind tunnel hub accelerations, the advance ratio, and $(C_T\cos\alpha_s)/\sigma$. The single output is the respective pilot floor vibration flight test value (flight test PVV or flight test PLATV or flight test PLONGV). For PVV, the above back-propagation network has been trained for 56,000 iterations with resulting R = 0.997 and RMS error = 0.002 g's. For PLATV, the above back-propagation network has been trained for 13,500 iterations with resulting R = 0.995 and RMS error = 0.001 g's. For PLONGV, the above back-propagation network has been trained for 45,000 iterations with resulting R = 0.995 and RMS error = 0.003 g's. The three correlation plots and the predictions for the three pilot floor vibration components are presented as follows.

PVV from wind tunnel hub accelerations. Figure 16a shows the correlation plot for the PVV using the measured wind tunnel hub accelerations. Figure 16b shows the representative, predicted PVV with advance ratio and the flight test PVV derived from Fig. 10. Figures 16a and 16b show that the three relevant measured wind tunnel hub accelerations and the operating parameters can characterize and quantify the low speed level flight PVV.

PLATV from wind tunnel hub accelerations. Figure 17a shows the correlation plot for the PLATV using the measured wind tunnel hub accelerations. Figure 17b shows the representative, predicted PLATV with advance ratio and the flight test PLATV derived from Fig. 11. Figures 17a and 17b show that the three relevant measured wind tunnel hub accelerations and the operating parameters can characterize and quantify the low speed level flight PLATV.

PLONGV from wind tunnel hub accelerations. Figure 18a shows the correlation plot for the PLONGV using the measured wind tunnel hub accelerations. Figure 18b shows the representative, predicted PLONGV with advance ratio and the flight test PLONGV derived from Fig. 12. Figures 18a and 18b show that the three relevant measured wind tunnel hub accelerations and the operating parameters can characterize and quantify the low speed level flight PLONGV.

Pilot vibration prediction using wind tunnel balance-system hub loads

Three different MISO 8-2-1 back-propagation neural networks are used (one for each of the three vibration components). The eight wind tunnel inputs are as follows: the six measured wind tunnel fixed system N/rev balance-system hub loads, the advance ratio, and $(C_T \cos\alpha_s)/\sigma$ (the latter two inputs are the same as the operating parameters). The single output is the respective pilot floor vibration flight test value (flight test PVV or flight test PLATV or flight test PLONGV). For PVV, the above back-propagation network has been trained for 13,400 iterations with resulting R = 0.997 and RMS error = 0.002 g's. For PLATV, the above back-propagation network has been trained for 3220 iterations with resulting R = 0.995 and RMS error = 0.001 g's. For PLONGV, the above back-propagation network has been trained for 5750 iterations with resulting R = 0.996 and RMS error = 0.002 g's. The three correlation plots and the predictions for the three pilot floor vibration components are presented as follows.

PVV from wind tunnel balance loads. Figure 19a shows the resulting correlation plot for the PVV. Figure 19b shows the representative, predicted PVV with advance ratio and the flight test PVV derived from Fig. 10. Figures 19a and 19b show that the six components of the measured wind tunnel N/rev balance-system hub loads and the operating parameters can represent the low speed level flight PVV.

PLATV from wind tunnel balance loads. Figure 20a shows the resulting correlation plot for the PLATV. Figure 20b shows the representative, predicted PLATV with advance ratio and the flight test PLATV derived from Fig. 11. Figures 20a and 20b show that the six components of the measured wind tunnel N/rev balance-system hub loads and the operating parameters can represent the low speed level flight PLATV.

PLONGV from wind tunnel balance loads. Figure 21a shows the resulting correlation plot for the PLONGV. Figure 21b shows the representative, predicted PLONGV with advance ratio and the flight test PLONGV derived from Fig. 12. Figures 21a and 21b show that the six components of the measured wind tunnel N/rev balance-system hub loads and the operating parameters can represent the low speed level flight PLONGV.

Concluding Remarks

Using only flight test data, it was shown earlier (Refs. 1 and 2) that neural networks can be used to connect the flight test rotating system hub accelerations to the flight test pilot floor vibration. The present neural network representation study introduces the use of full-scale wind tunnel test data to model the flight test pilot floor vibration. This study considers the three peak, N/rev components of the flight test pilot floor vibration in low speed level flight. Specific conclusions from this study are as follows:

1) The wind tunnel rotating hub accelerations and operating parameters can be used to represent the low speed pilot floor vibration.

2) The wind tunnel fixed-system N/rev hub loads and the operating parameters can also be used to represent the low speed pilot floor vibration.

3) Based on the above conclusions, it appears that the wind tunnel rotating system hub accelerations can have a significant role since they can be used to represent the pilot floor vibration. In order to model the pilot floor vibration, compared to the use of the fixed system balance-system hub loads, the successful use of the rotating system hub accelerometers may entail less effort. This would be because the use of a fixed system balance-system would involve the associated calibration of the balance (which in the present case was calibrated using a static procedure). However, at the same time, good results have been presently obtained using the hub loads without the dynamic calibration of the balance, i.e., good "R's" have been obtained with only static calibration of the balance.

In general, the successful establishment of neural network based connections between the wind tunnel parameters and the flight test data (such as the connections that have been initiated in the present study) can significantly increase the value of wind tunnel testing.

References

1. Kottapalli, S., "Neural Network Based Representation of UH-60A Pilot and Hub Accelerations," *Journal of the American Helicopter Society*, Vol. 47, (1), January 2002, pp. 33-41.

2. Kottapalli, S., "Modeling of UH-60A Hub Accelerations with Neural Networks," American Helicopter Society Aerodynamics, Acoustics, and Test and Evaluation Technical Specialists' Meeting, San Francisco, California, January 23-25, 2002.

3. Kottapalli, S. and Campbell, R., "Modeling of UH-60A Pilot Vibration Using Neural Networks and Wind Tunnel Data," International Forum on Aeroelasticity and Structural Dynamics 2003 (IFASD 2003), Amsterdam, The Netherlands, June 4-6, 2003, Paper No. US-21.

4. Kufeld, R.M. and Bousman, W.G., "UH-60A Helicopter Rotor Airloads Measured in Flight," *The*

Aeronautical Journal of the Royal Aeronautical Society, May 1997.

5. Norman, T. R., Shinoda, P. M., Jacklin, S. A., and Sheikman, A., "Low-Speed Wind Tunnel Investigation of a Full-Scale UH-60 Rotor System," Proceedings of the 58th Annual Forum of the American Helicopter Society, Montreal, Canada, June 11-13, 2002.

6. Jacklin, S. A., Haber, A., de Simone, G., Norman, T. R., Kitaplioglu, C., and Shinoda, P. M., "Full-Scale Wind Tunnel Test of an Individual Blade Control System for a UH-60 Helicopter," Proceedings of the 58th Annual Forum of the American Helicopter Society, Montreal, Canada, June 11-13, 2002.

7. Shinoda, P., Yeo, H., and Norman, T.R., "Rotor Performance of a UH-60 Rotor System in the NASA Ames 80- by 120-Foot Wind Tunnel," Proceedings of the 58th Annual Forum of the American Helicopter Society, Montreal, Canada, June 11-13, 2002.

8. NeuralWorks Professional II/PLUS Manuals: a) Reference Guide b) Neural Computing c) Using NeuralWorks, NeuralWare, Inc., Pittsburgh, Pennsylvania, 1995.

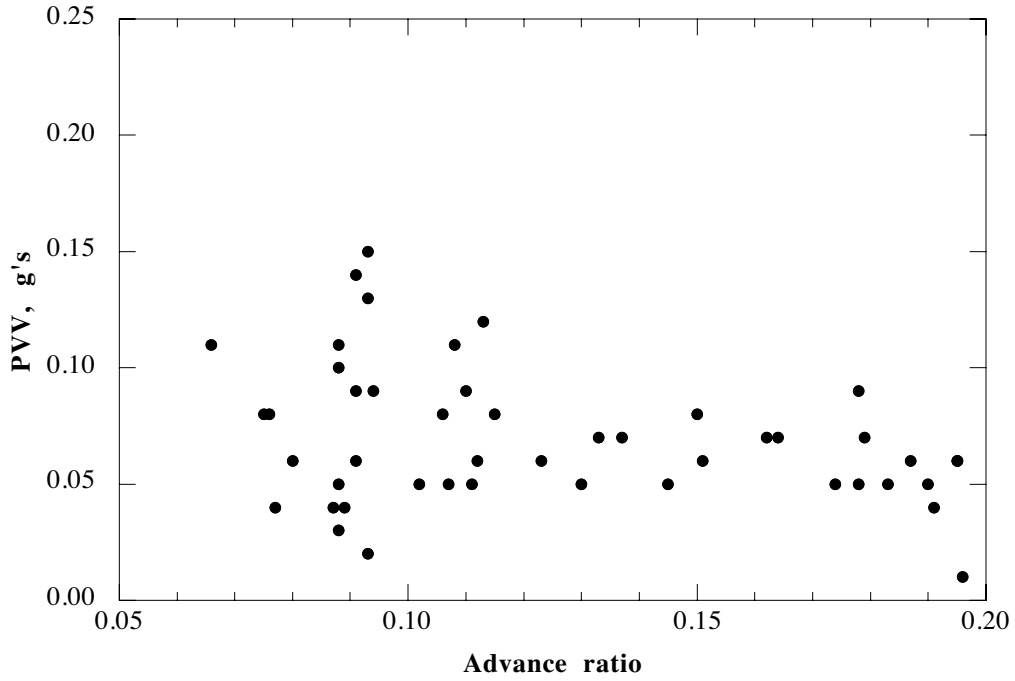

Fig. 1. UH-60A peak, N/rev pilot floor vertical vibration, PVV, variation with advance ratio.

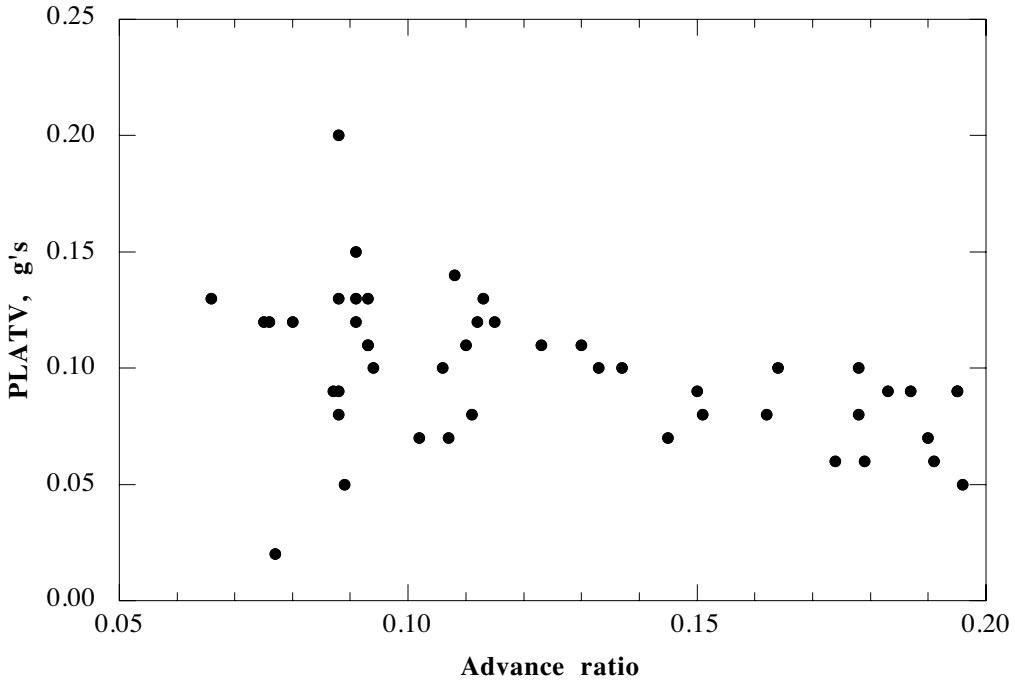

Fig. 2. UH-60A peak, N/rev pilot floor lateral vibration, PLATV, variation with advance ratio.

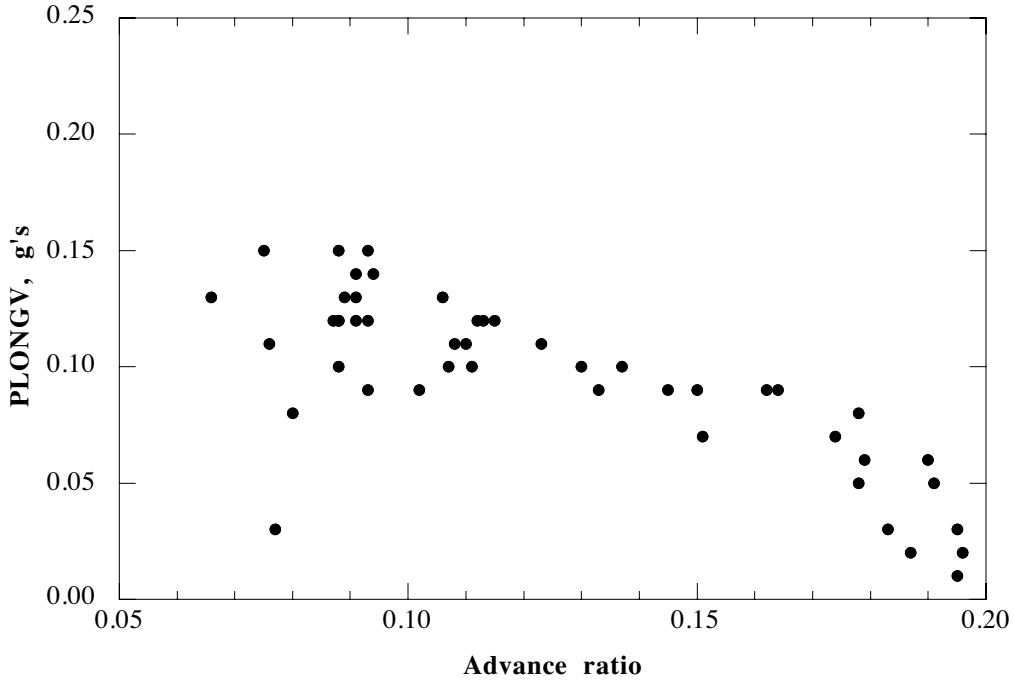

Fig. 3. UH-60A peak, N/rev pilot floor longitudinal vibration, PLONGV, variation with advance ratio.

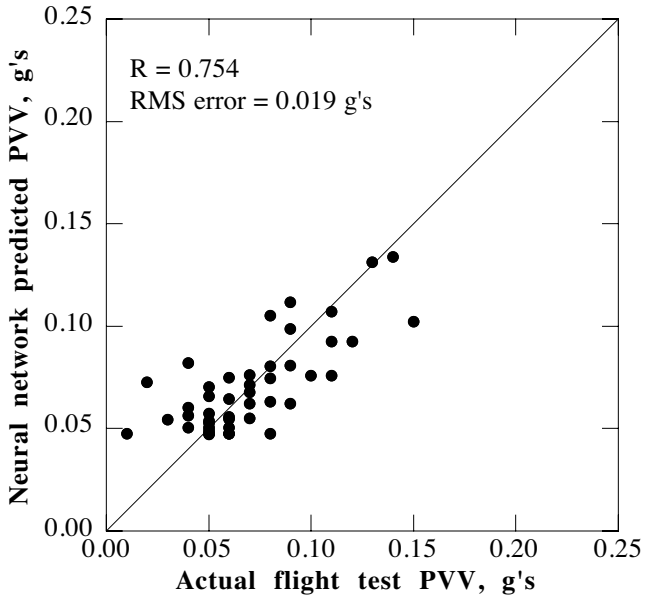

Fig. 4. PVV correlation using advance ratio and gross weight.

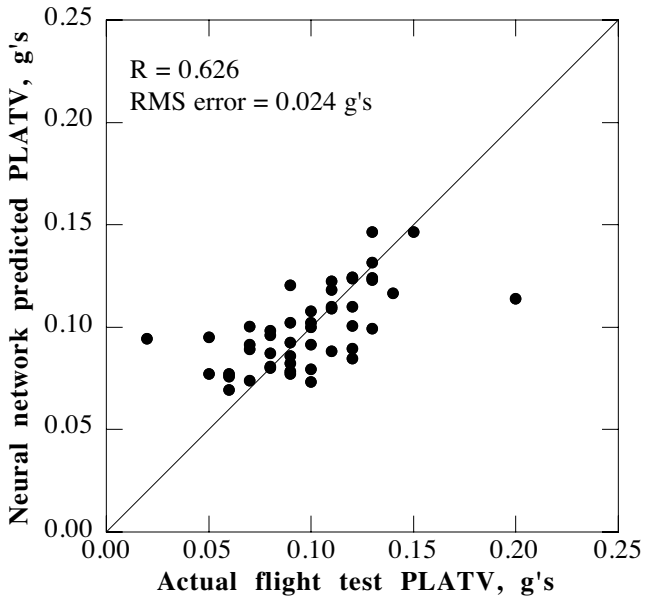

Fig. 5. PLATV correlation using advance ratio and gross weight.

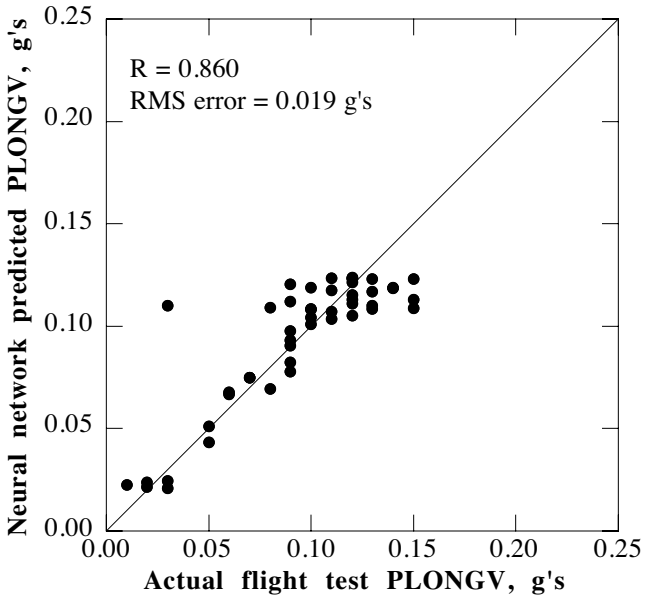

Fig. 6. PLONGV correlation using advance ratio and gross weight.

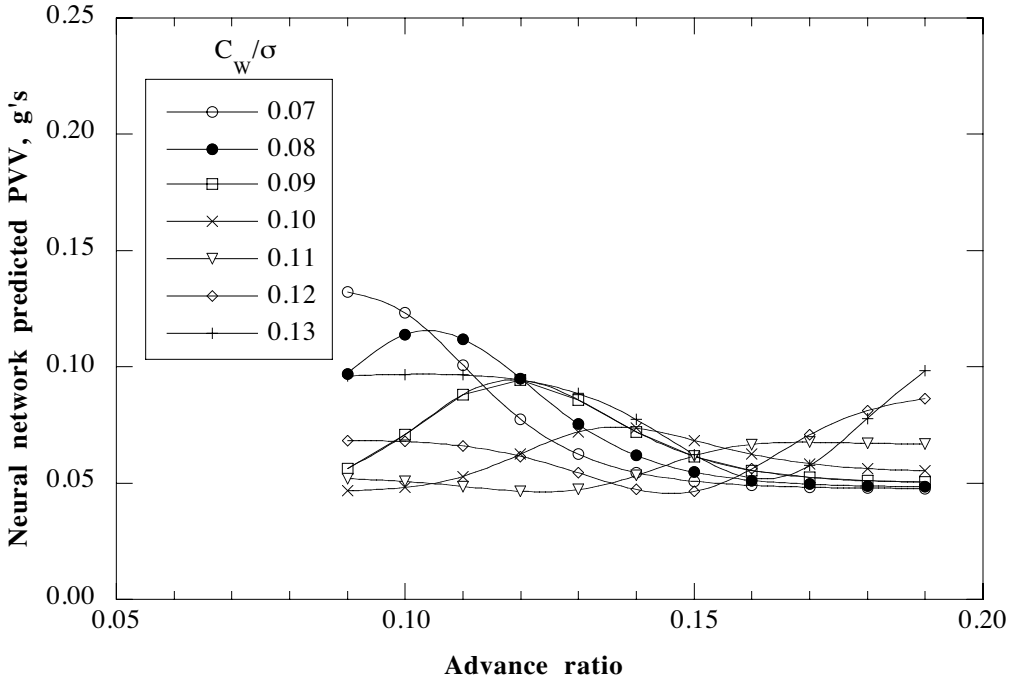

Fig. 7. Predicted PVV trends using advance ratio and gross weight.

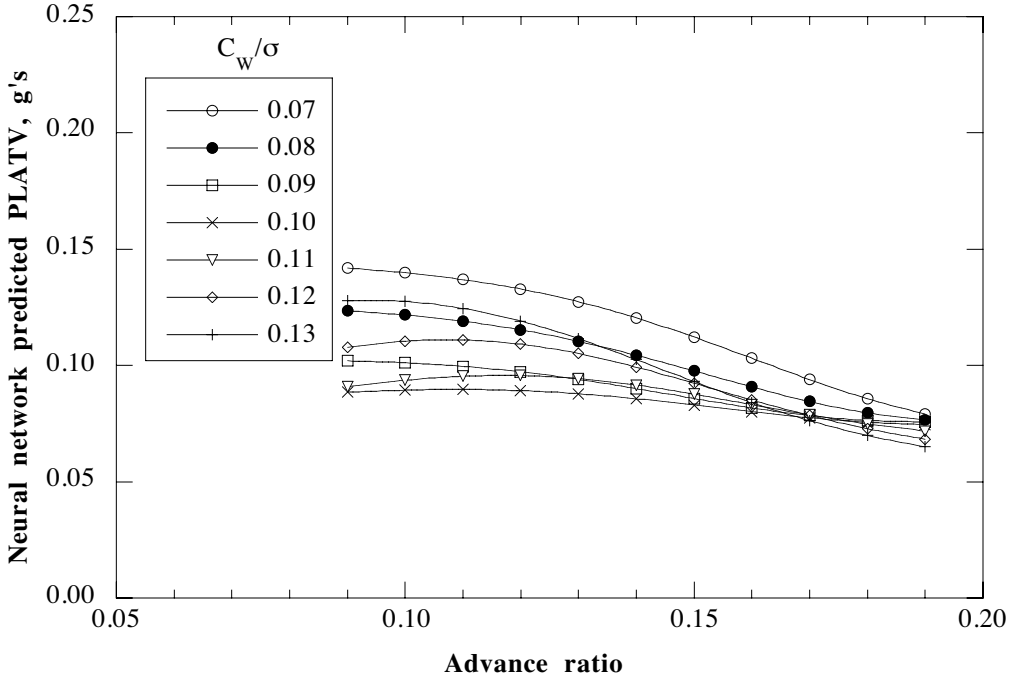

Fig. 8. Predicted PLATV trends using advance ratio and gross weight.

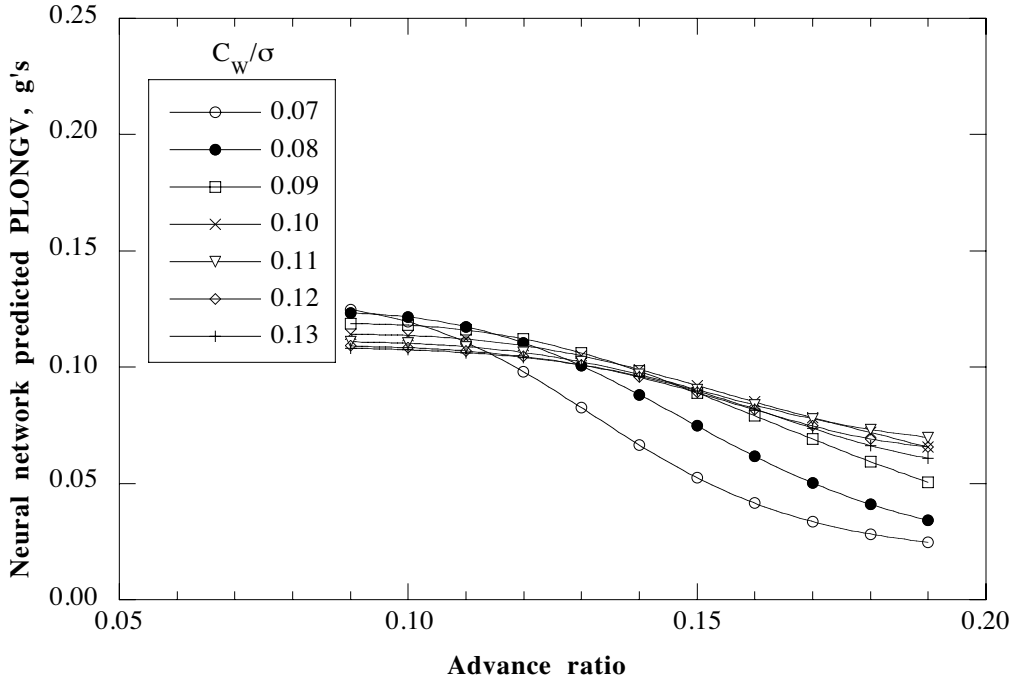

Fig. 9. Predicted PLONGV trends using advance ratio and gross weight.

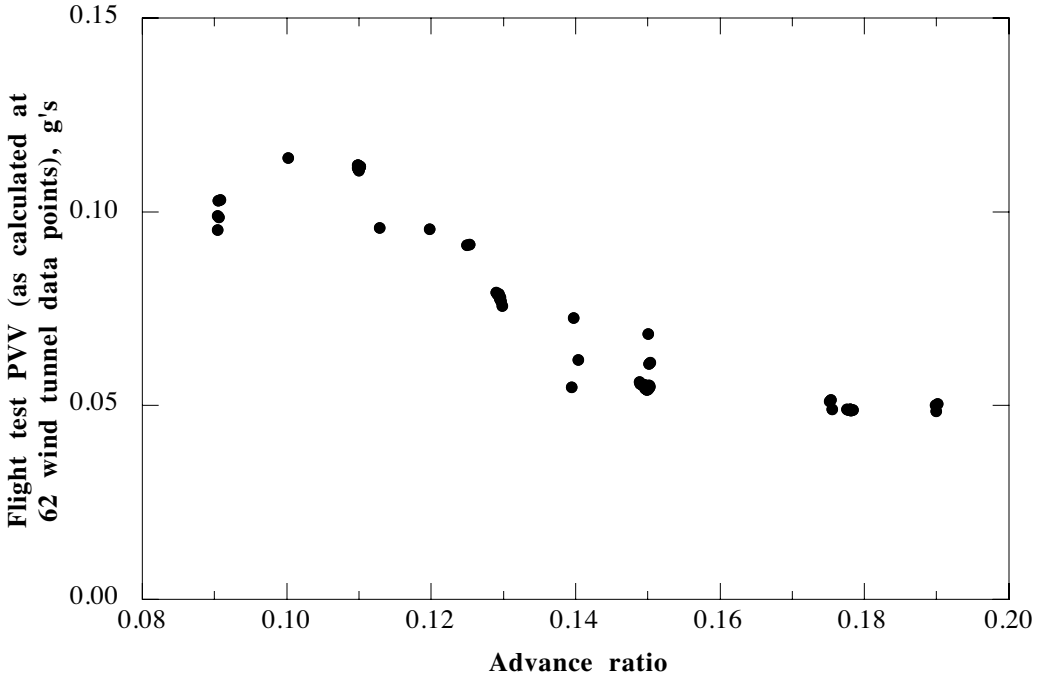

Fig. 10. Predicted flight test PVV using advance ratio and gross weight, evaluated at 62 wind tunnel data points, includes thrust variations.

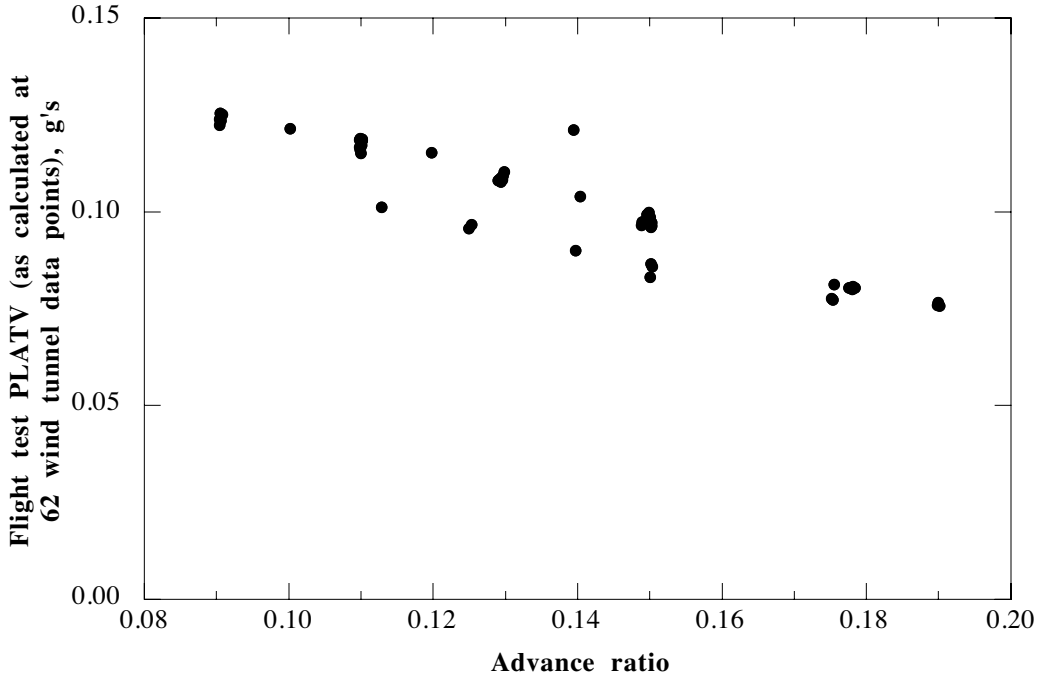

Fig. 11. Predicted flight test PLATV using advance ratio and gross weight, evaluated at 62 wind tunnel data points, includes thrust variations.

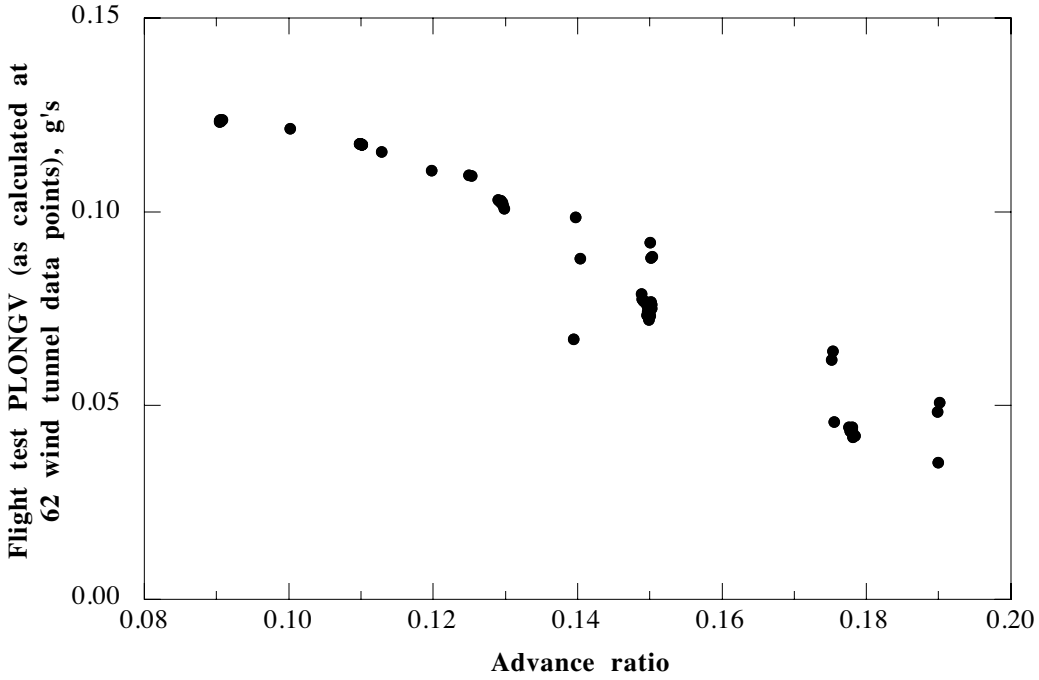

Fig. 12. Predicted flight test PLONGV using advance ratio and gross weight, evaluated at 62 wind tunnel data points, includes thrust variations.

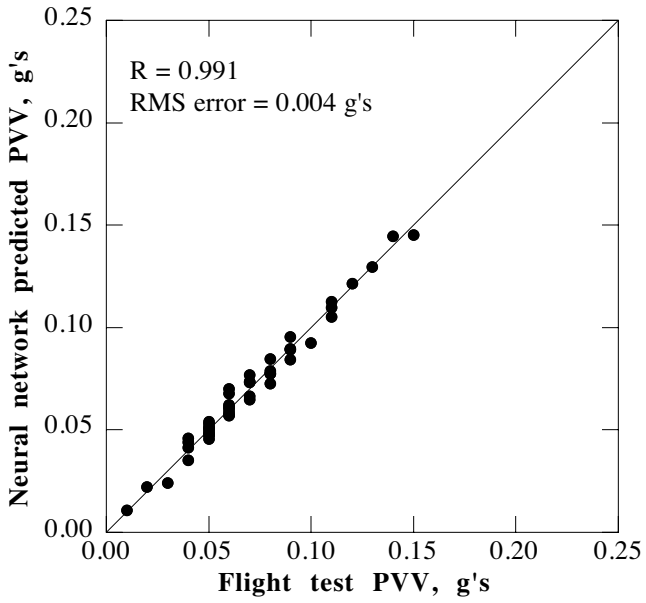

Fig. 13a. PVV correlation using flight test rotating system hub accelerations and operating parameters.

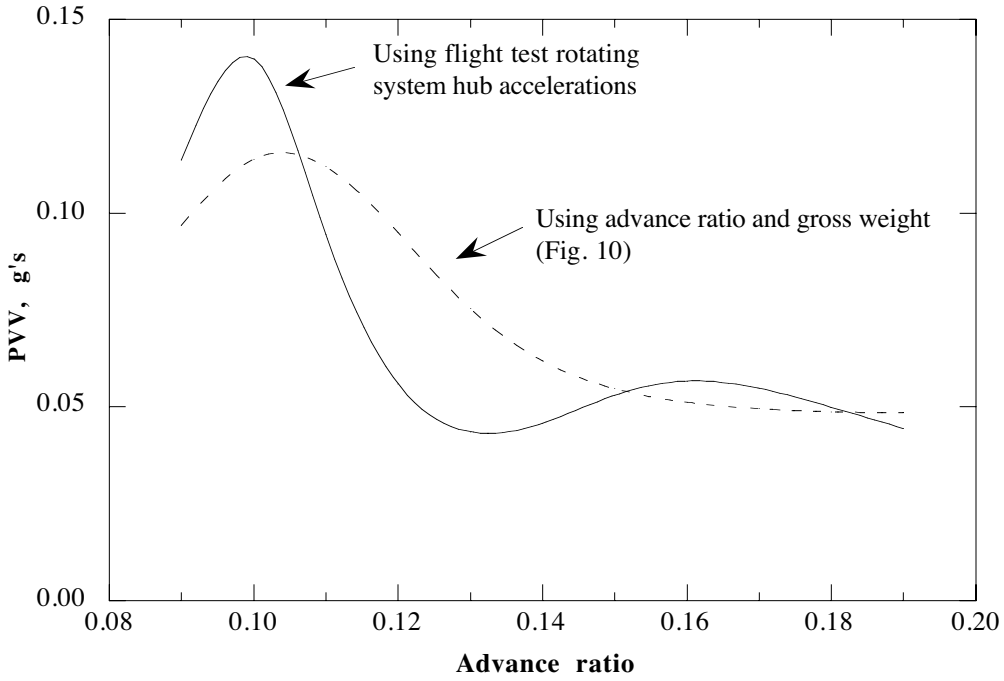

Fig. 13b. PVV prediction using flight test rotating system hub accelerations and operating parameters (C_W/σ = 0.08).

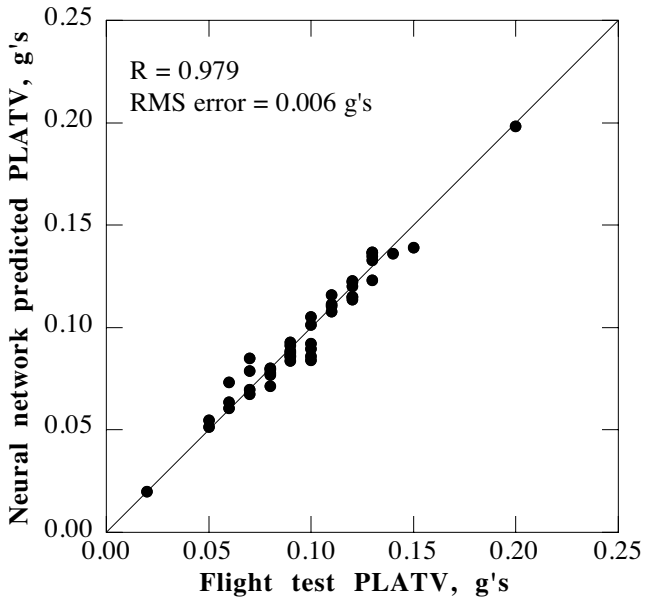

Fig. 14a. PLATV correlation using flight test rotating system hub accelerations and operating parameters.

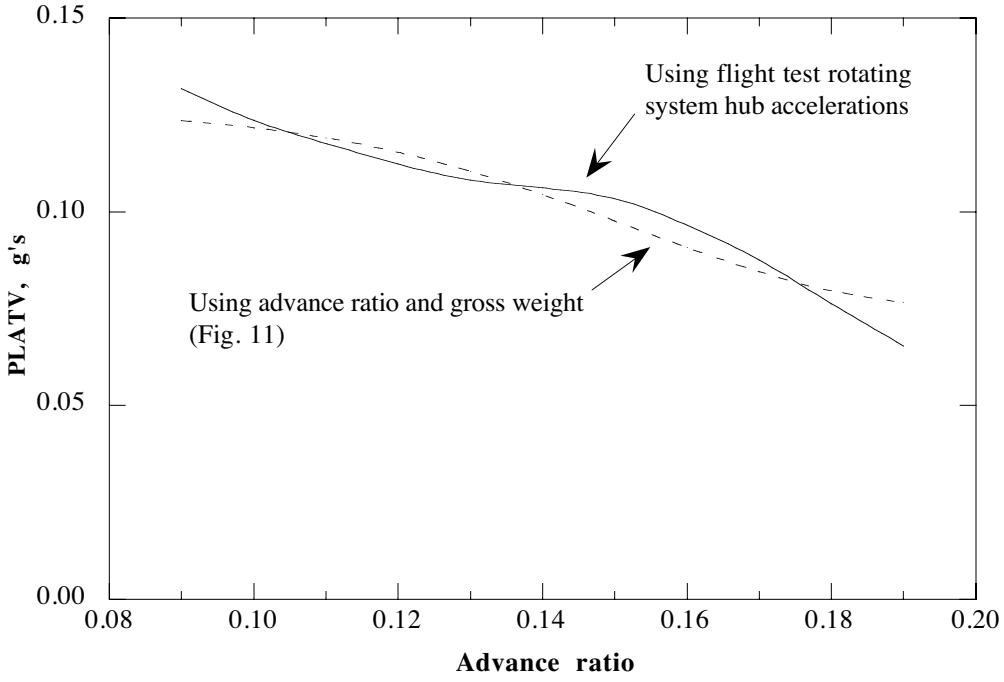

Fig. 14b. PLATV prediction using flight test rotating system hub accelerations and operating parameters (C_W/σ = 0.08).

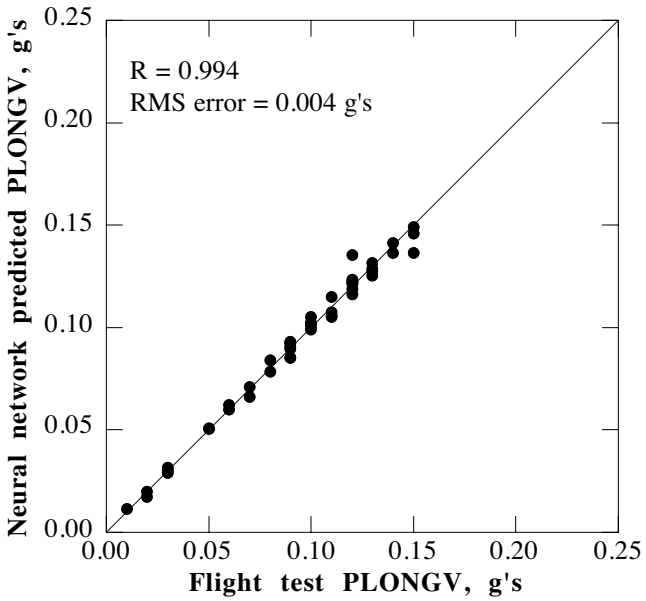

Fig. 15a. PLONGV correlation using flight test rotating system hub accelerations and operating parameters.

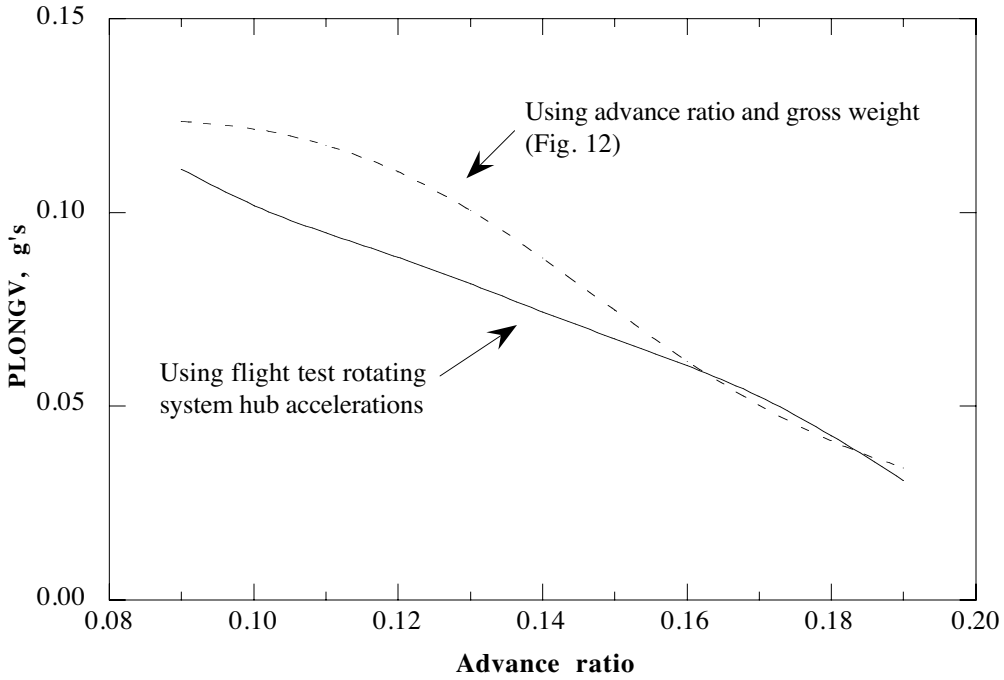

Fig. 15b. PLONGV prediction using flight test rotating system hub accelerations and operating parameters (C_W/σ = 0.08).

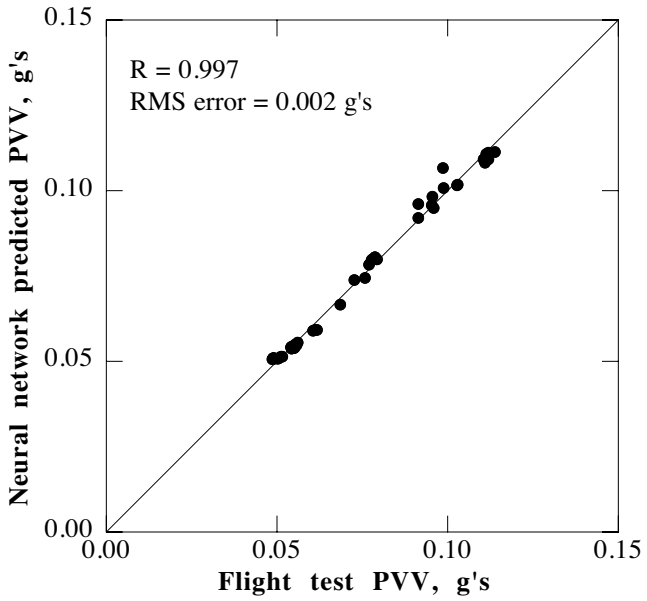

Fig. 16a. PVV correlation using wind tunnel rotating system hub accelerations and operating parameters.

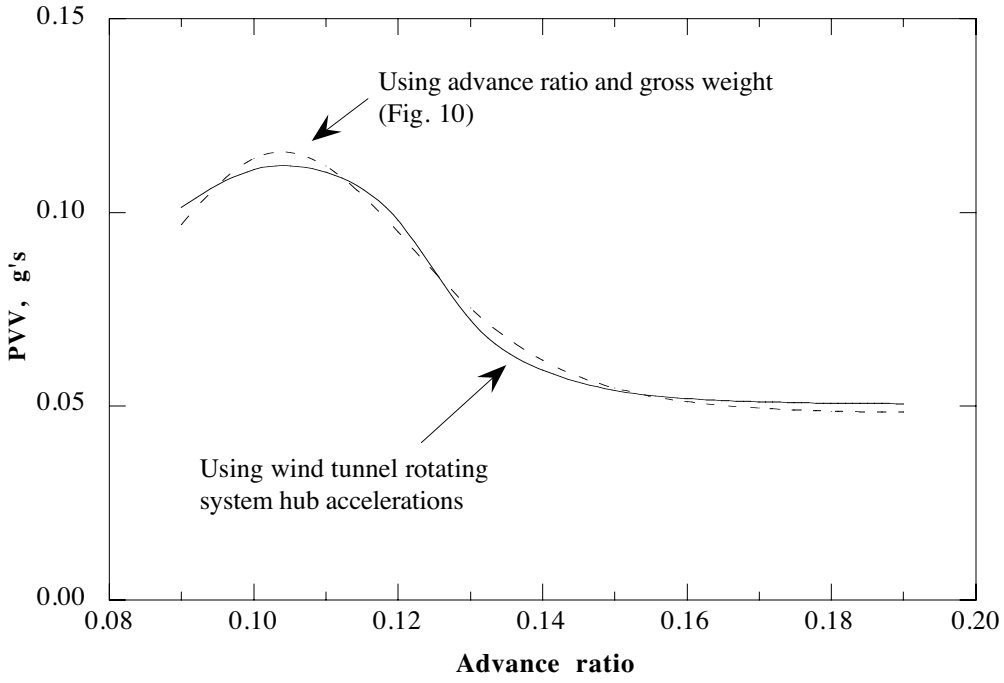

Fig. 16b. PVV prediction using wind tunnel rotating system hub accelerations and operating parameters (C_W/σ = 0.08).

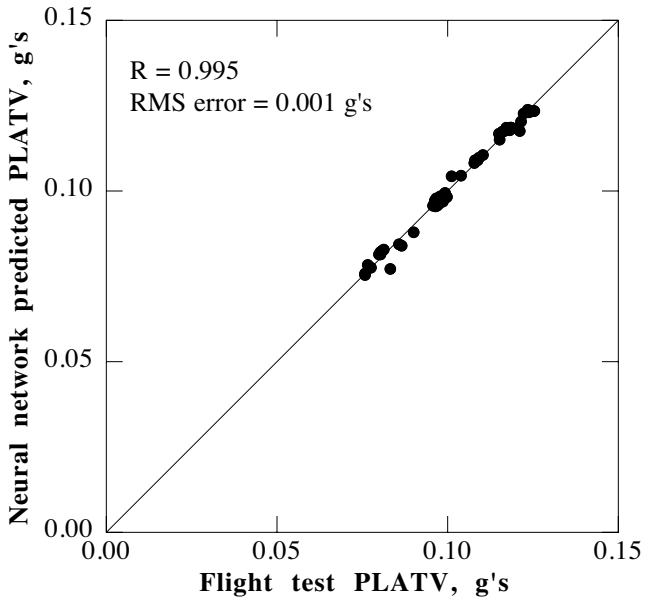

Fig. 17a. PLATV correlation using wind tunnel rotating system hub accelerations and operating parameters.

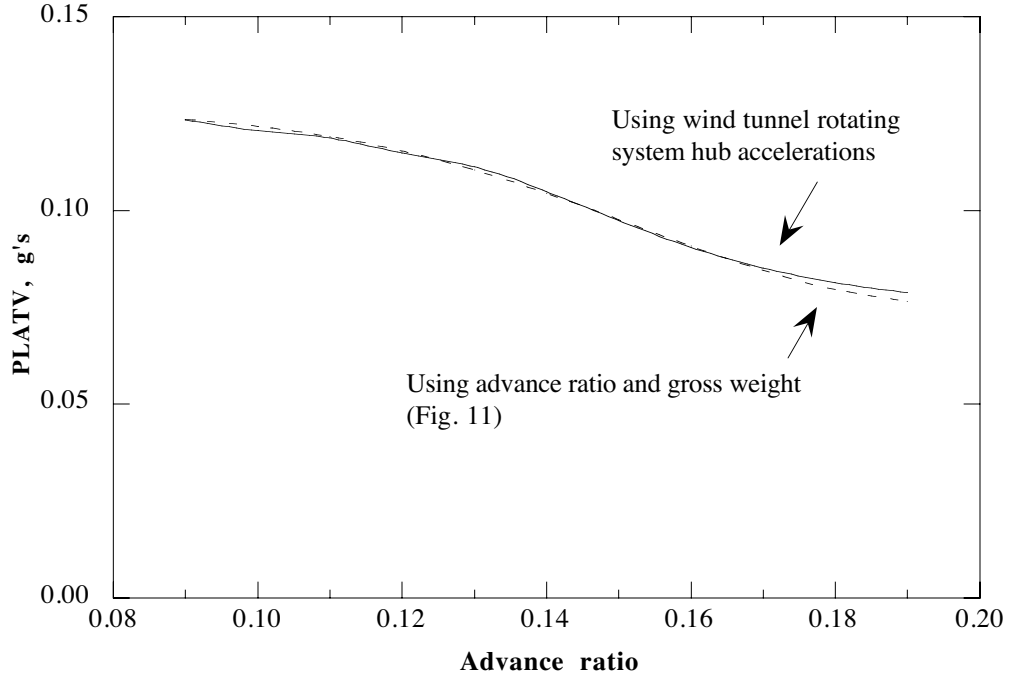

Fig. 17b. PLATV prediction using wind tunnel rotating system hub accelerations and operating parameters (C_W/σ = 0.08).

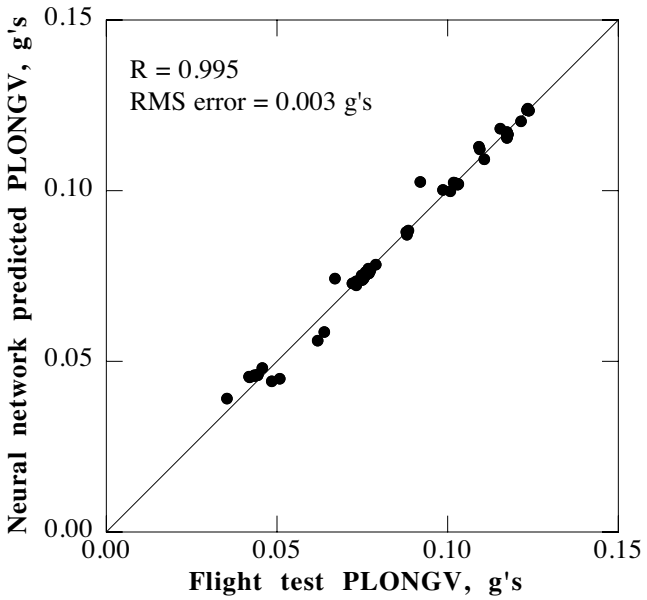

Fig. 18a. PLONGV correlation using wind tunnel rotating system hub accelerations and operating parameters.

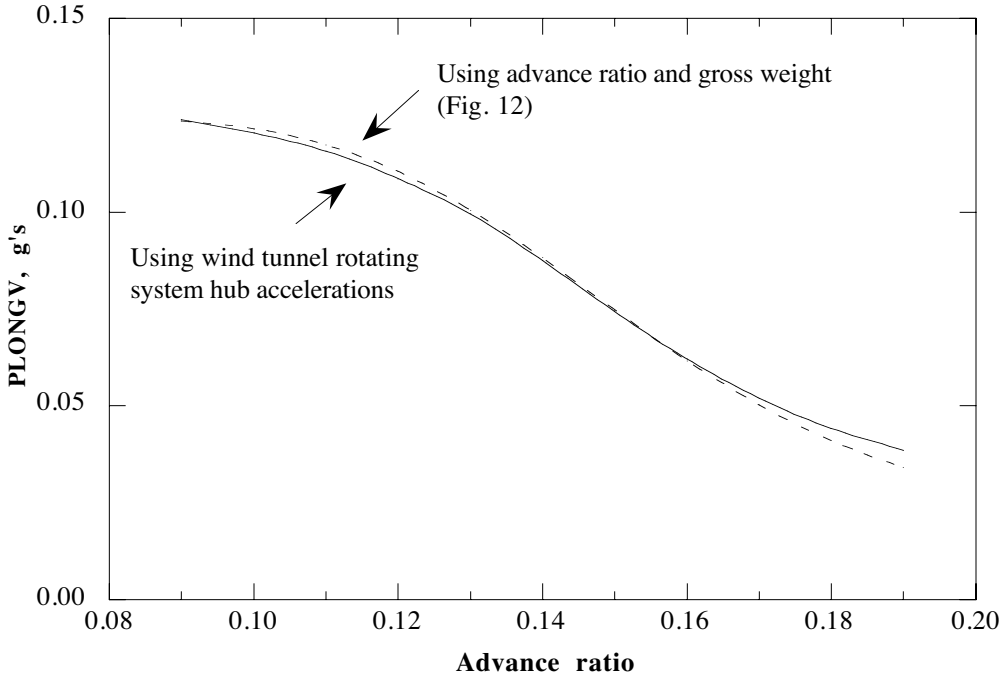

Fig. 18b. PLONGV prediction using wind tunnel rotating system hub accelerations and operating parameters (C_W/σ = 0.08).

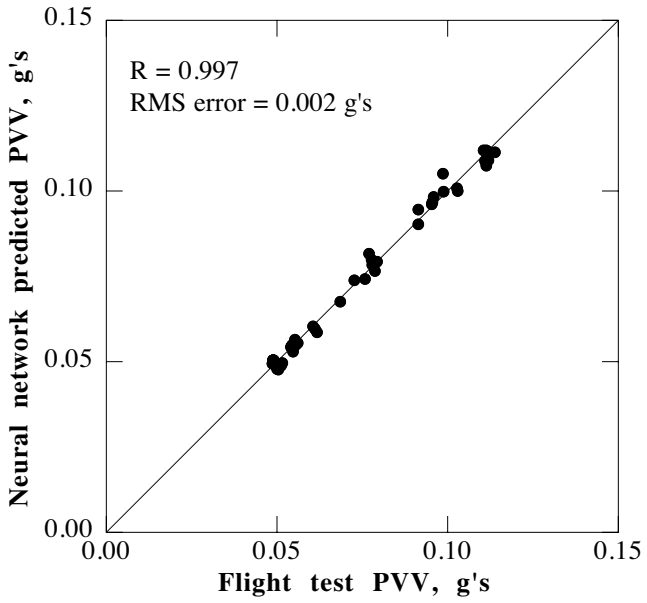

Fig. 19a. PVV correlation using six components of N/rev balance-system hub loads and operating parameters.

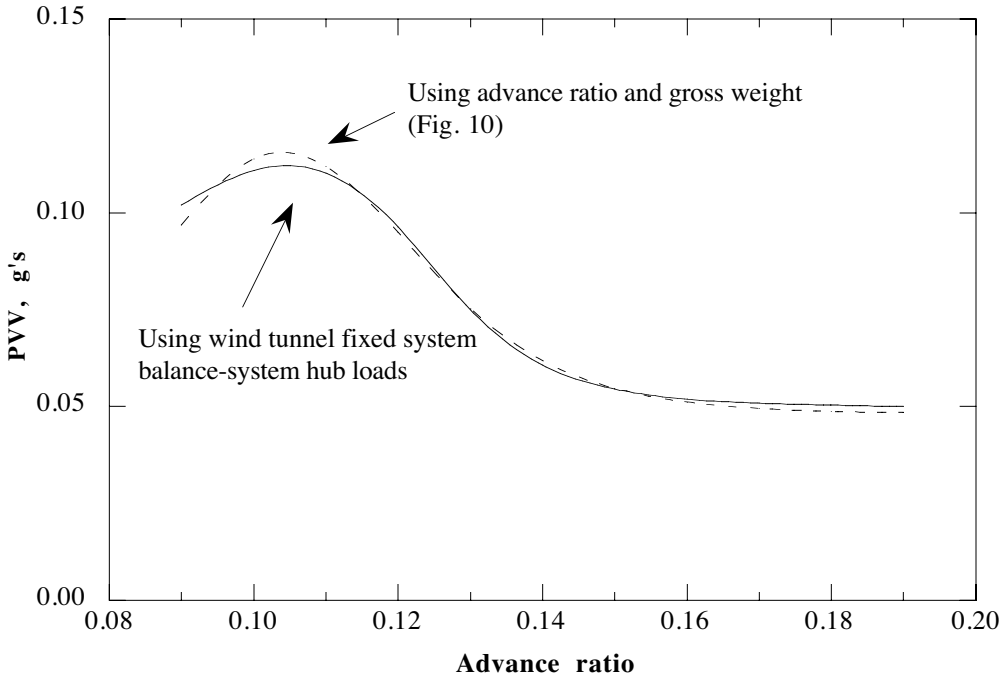

Fig. 19b. PVV prediction using six components of N/rev balance-system hub loads and operating parameters (C_W/σ = 0.08).

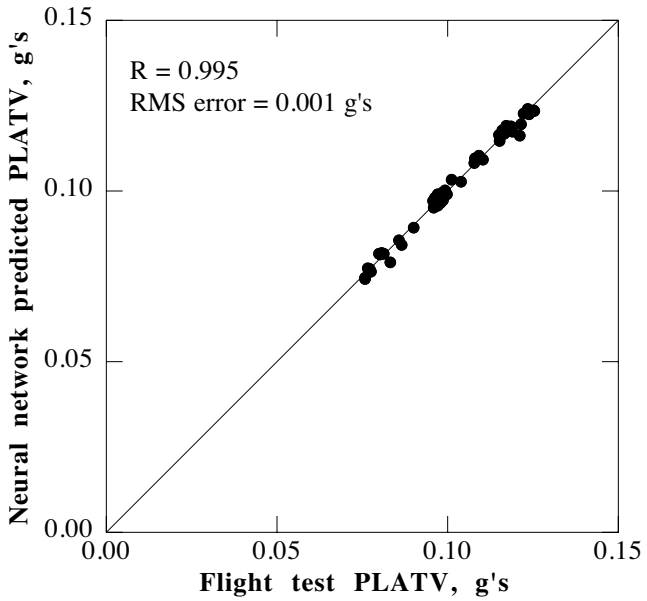

Fig. 20a. PLATV correlation using six components of N/rev balance-system hub loads and operating parameters.

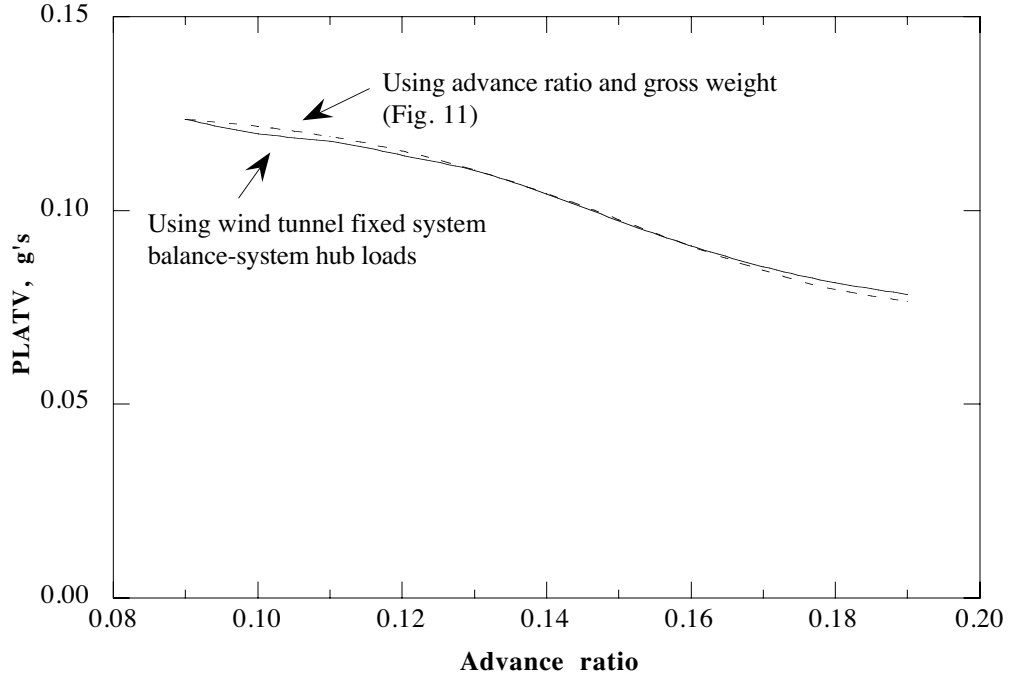

Fig. 20b. PLATV prediction using six components of N/rev balance-system hub loads and operating parameters (C_W/σ = 0.08).

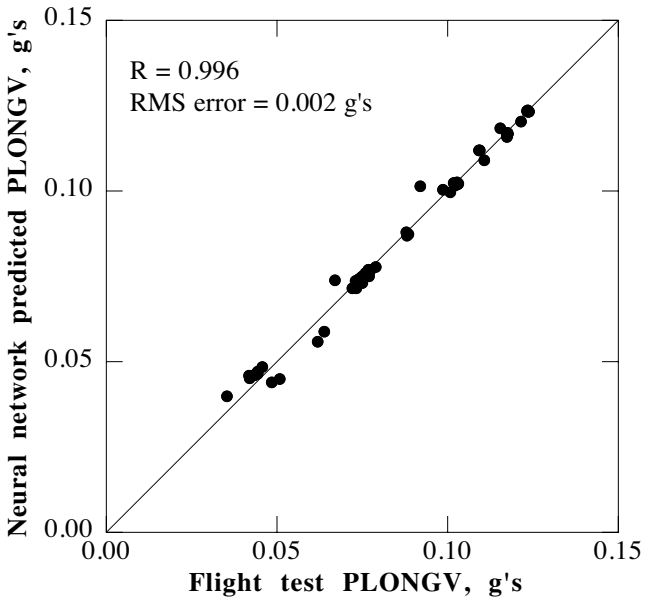

Fig. 21a. PLONGV correlation using six components of N/rev balance-system hub loads and operating parameters.

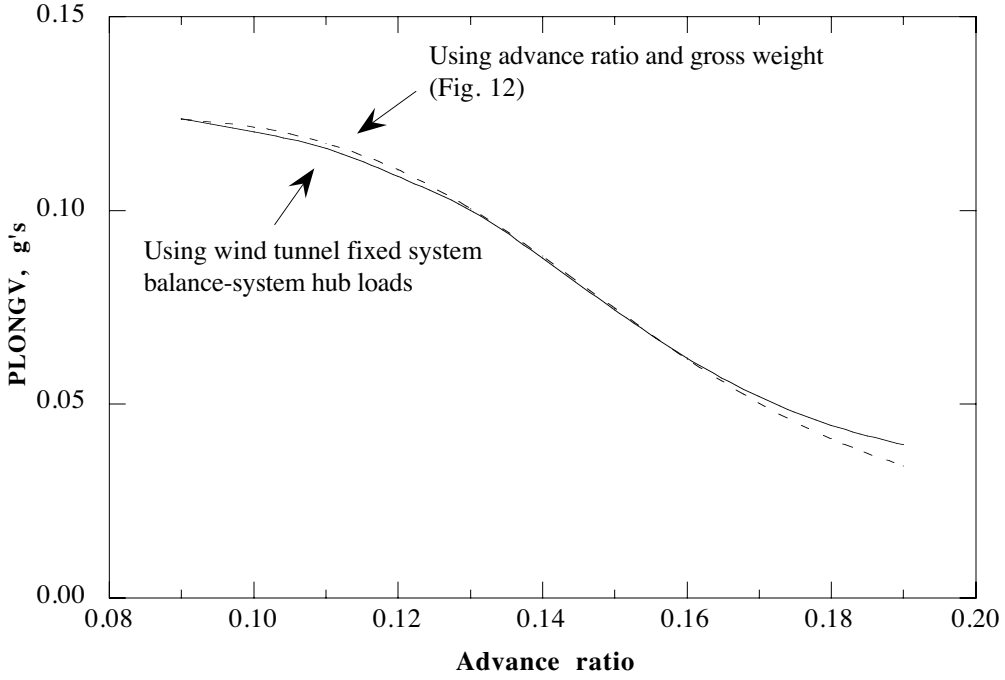

Fig. 21b. PLONGV prediction using six components of N/rev balance-system hub loads and operating parameters (C_W/σ = 0.08).